

Interference Mitigation in Passive Microwave Radiometry

A.J. Gasiewski¹, M. Klein², A. Yevgrafov², V. Leuskiy²

¹ NOAA Environmental Technology Laboratory, R/E/ET1, 325 Broadway, Boulder, CO 80305.
e-mail: al.gasiewski@noaa.gov, tel: + 303 497-7275, fax: + 303 497-3577

² CIRES, University of Colorado/NOAA Environmental Technology Laboratory, R/E/ET1, 325 Broadway, Boulder, CO 80305. e-mail: marian.klein@noaa.gov, tel: +1 303 497-6418, fax: +1 303 497-3577, e-mail: aleksandr.yevgrafov@noaa.gov, tel: +1 303 497-7075, e-mail: vladimir.leuskiy@noaa.gov, tel: +1 303 497-6937

Abstract - Relentless development of the microwave spectrum for telecommunications and other active services enhances the risk of anthropogenic interference to the passive Earth Exploration Satellite Service (EESS). While spectral allocation remains the primary basis for avoiding interference between the passive and active services, it is also prudent to consider the use of interference mitigation technology for passive microwave remote sensing, especially for spectral regions wherein primary EESS allocation is non-negotiable. Accordingly, we consider several means of detecting and correcting for anthropogenic interference in passive microwave imagery, including spectral subbanding, polarization detection, polarimetric detection, and azimuthal detection. A spectral subband technique applicable to either narrow-band and/or window channels is demonstrated with C-band data obtained using the NOAA Polarimetric Scanning Radiometer (PSR) airborne imaging system. The technique provides very good rejection of strong interference, and is readily applicable for implementation on future airborne and spaceborne passive microwave sensors.

I. INTRODUCTION

The widespread use of microwave bands for telecommunications and other active purposes has resulted in the loss of much quiet spectrum previously available for passive Earth remote sensing. Although a series of bands have been allocated by the International Telecommunications Union (ITU) specifically for the passive Earth Environmental Satellite Service (EESS) and related airborne and ground-based remote sensing activities, these bands do not cover all of the necessary spectral ranges. In addition, the allocated bands provide no more than statutory protection, with absolute insurance against interference from accidental out-of-band emissions to intentional jamming being all but impractical. Means of detecting and correcting for interfering signals in passive remote sensing of natural planetary emissions are thus becoming increasingly important, particularly as requirements are identified for detecting small climate change signatures using passive microwave systems.

Interference mitigation algorithms can exploit certain common features of anthropogenic signals that cause them to be distinguishable from natural planetary emission. These features include: 1) a narrowband spectrum relative to the bandwidth of commonly used passive microwave bands, 2) an unusually high degree of slant-linear polarization, 3) an unusually high degree of polarization correlation, and 4) a high degree of directional anisotropy. We can associate with

these four features four basic methods for interference mitigation: 1) subband diversity, 2) polarization diversity, 3) polarimetric detection, and 4) azimuthal diversity. Each of the above methods provides the possibility of detecting interference, although the first (subband diversity) also provides a means of correcting for interference.

We demonstrate in this paper the first of these four basic methods of interference mitigation. A robust subband diversity algorithm was developed and tested using data from the NOAA Polarimetric Scanning Radiometer C-band (PSR/C) airborne imaging system [1]. The PSR/C was flown on the NASA P-3 aircraft as part of the 1999 Southern Great Plains experiment (SGP99), yielding the first high-resolution (~2x3 km) C-band polarimetric imagery of soil moisture variations. The data from the PSR over the area near Oklahoma City clearly show 50-70 K changes in upwelling horizontally-polarized brightness temperature as the result of variations in soil moisture [2], although anthropogenic interference at C-band is also common. A spectral interference correction algorithm using four subbands was developed and applied to this data. The algorithm provided almost complete correction of the PSR/C imagery along with maps of interference severity that are anticipated to be useful for a variety of subsequent user applications.

While certainly not as desirable as clean protected spectrum, interference mitigation techniques that exploit the features of anthropogenic emission are expected to be valuable, particularly within bands where primary EESS spectral allocations do not exist. Spatial, polarization-based, and polarimetric interference detection also appear to be potentially useful.

II. BASIC SPECTRAL MITIGATION ALGORITHM

Figure 1 illustrates the basic spectral mitigation algorithm for four subbands and a linear spectral model. The spectral model is selected to be capable of simulating all of the significant spectral behavior of "clean" T_B spectra over the band of interest. A linear spectral model is thus a reasonable choice for most microwave window or narrowband sounding channels, while an absorption line model based on, e.g., the Van Vleck-Weisskopf line shape superimposed on a linear model would be more suitable for a wideband oxygen or water vapor channel. The number of subbands within the band of interest must be significantly larger than the number

of degrees of freedom in the model plus the expected number of “spectrally-distinct” interfering sources. A four-subband linear model can thus be expected to provide good correction for at most one interfering source. Multiple interfering sources that fall with a single subband constitute a single distinct source and are thus also able to be accommodated.

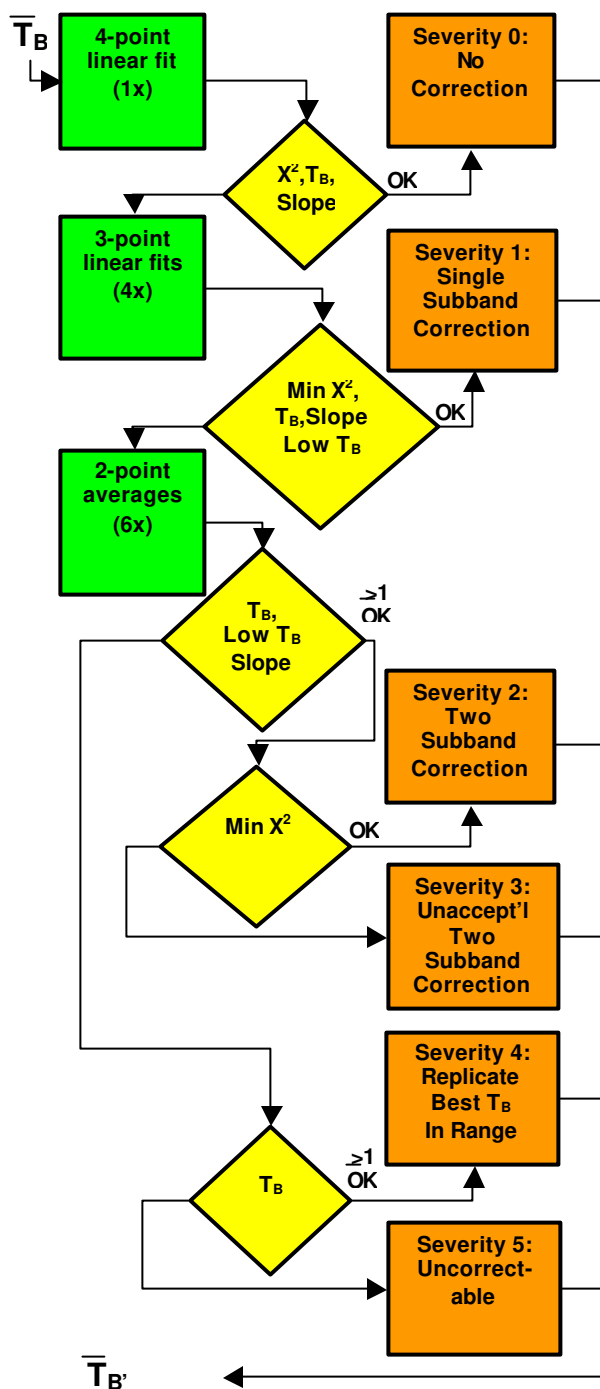


Figure 1. Block diagram of the basic spectral interference mitigation and correction algorithm for narrowband and/or window channels. The algorithm assumes the use of four uniformly distributed spectral subbands.

The algorithm proceeds by performing a standard least squares spectral fit, then analyzing both the χ^2 parameter for fit goodness ($\chi^2 > N-M$, where N is the number of subbands and M is the number of degrees of freedom in the spectral model) and the best fit coefficients for physical plausibility. Here, the noise standard for the calculation of χ^2 includes both radiometric and geophysical contributions. If the fit is good and all parameters are within a-priori bounds then no corrections are performed, else the spectral fit is reiterated once for each subband under the condition that data from that subband is deleted from the fit process. The process is continued by removing additional subbands until a subband combination is found providing both a good fit (using the χ^2 parameter) and all fit parameters are within physical bounds.

It should be noted that the placement of the subbands need not be uniformly distributed across the band of interest, but could be weighted more heavily in a region of higher than normal expected interference. Similarly, the set of bands need not be non-overlapping. Such subband asymmetries must, however, be properly accounted for within the model parameter estimation process.

At each level of modeling and/or correction an interference severity code is assigned (0-5 for the four subband case). This code indicates the degree of correction and can be used to flag interference as well as provide a measure of data quality for use in ensuing retrieval or assimilation operations.

III. DEMONSTRATION USING AIRCRAFT DATA

In an effort to provide brightness data necessary to develop soil moisture retrieval algorithms in support of the NASA Aqua Advanced Microwave Scanning Radiometer (AMSR-E) brightness imagery over a wide area of central Oklahoma was obtained using the PSR/C during SGP99 on six days in July, 1999. The PSR/C C-band radiometer was implemented using four adjacent and near-uniformly distributed subbands at 5.80-6.20, 6.30-6.70, 6.75-7.10, and 7.15-7.50, each with vertical and horizontal polarization. The third of these subbands (corresponding to the AMSR-E C-band channel) also provided third and fourth Stokes parameter measurements. The instrument was operated in conically-scanned mode at 55° incidence from nadir.

Strong isolated regions of anthropogenic interference of up to ~ 1000 K were repeatedly observed at several locations within the $\sim 50 \times 270$ km multiple-swath image. Interference is obvious in all subbands (including the AMSR-E band) although least prevalent within 7.15-7.50 GHz. Figure 2a shows a representative portion of one of four parallel swaths observed on July 14, 1999. Saturation of the PSR/C front-end amplifiers was ruled out as possible cause of the interference since the occurrences are not well correlated across the subbands. The sources of interference appeared to be fixed-point microwave communications links, although transmitters were unambiguously identified in only a few occurrences.

The spectral subband algorithm was applied to each PSR/C multiband brightness vector using the following parameters:

$\Delta T_{RMS+GEO}=2.5K$, a maximum acceptable spectral slope of 7 K/GHz, and conservative brightness thresholds of 190-310 K for V-pol and 130-310 K for H-pol. The corrected imagery (Figure 2b) is largely free from obvious sources of interference, and readily useful for soil moisture retrieval.

We note that the application of polarization/polarimetric detection and azimuthal detection stands to further improve interference detection (and hence correction). Demonstrations of these techniques are currently in progress at NOAA/ETL.

IV. DISCUSSION

Anthropogenic emission in several key microwave bands, most notably L, C, X, Ku, Ka, and V, increasingly threatens the ability to conduct passive microwave environmental remote sensing research and operations. Only small amounts of interfering power are necessary to corrupt environmental data, with the worst case occurring for interference power levels that are indistinguishable from the system thermal emission, sensitivity limit, i.e., $\Delta P_{INT} \sim k\Delta T_{RMS}$ with $\sim 0.1 < \Delta T_{RMS} < \sim 10$ K. Persistent undetected interference is expected to have adverse impacts on microwave radiometer-based climate records and long term weather forecasts. Passive radio band allocations are critical to prevent interference, but even primary allocations may be no guarantee of long-term immunity.

This work demonstrates that for microwave window and/or

narrow band channels in which passive microwave systems suffer strong interference that very good detection and correction can be obtained using spectral subbanding. Unfortunately, the currently available aircraft observations suggest that C-band channels on the AMSR-E and WINDSAT sensors will likely suffer at least some interference over land. The results of this work suggest, however, that future sensors - such as the NPOESS Conical Microwave Imager/Sounder - can be readily modified to provide an enhanced degree of interference detection and correction using the spectral subband technique.

ACKNOWLEDGEMENTS

The authors acknowledge the contributions of S. Christiani and S. Jordan to the calibration and processing of the PSR SGP99 data. This work was supported by NOAA/OAR, USDA, and the NPOESS Integrated Program Office.

REFERENCES

- [1] M. Klein, A.J. Gasiewski, V. Irisov, A. Yevgrafov, V. Leuskiy, and P. Kimball, "A Wideband Airborne Microwave Imaging System for Hydrological Studies," *Proceedings of the International Geoscience and Remote Sensing Symposium*, Piscataway, NJ, IEEE, 2002.
- [2] Jackson, T.J., A.J. Gasiewski, A. Oldak, M. Klein, E.G. Njoku, A. Yevgrafov, S. Christiani, and R. Bindlish, "Soil Moisture Retrieval using the Cband Polarimetric Scanning Radiometer During the Southern Great Plains 1999 Experiment," accepted for publication in *IEEE Trans. Geosci. Remote Sensing*, February, 2002.

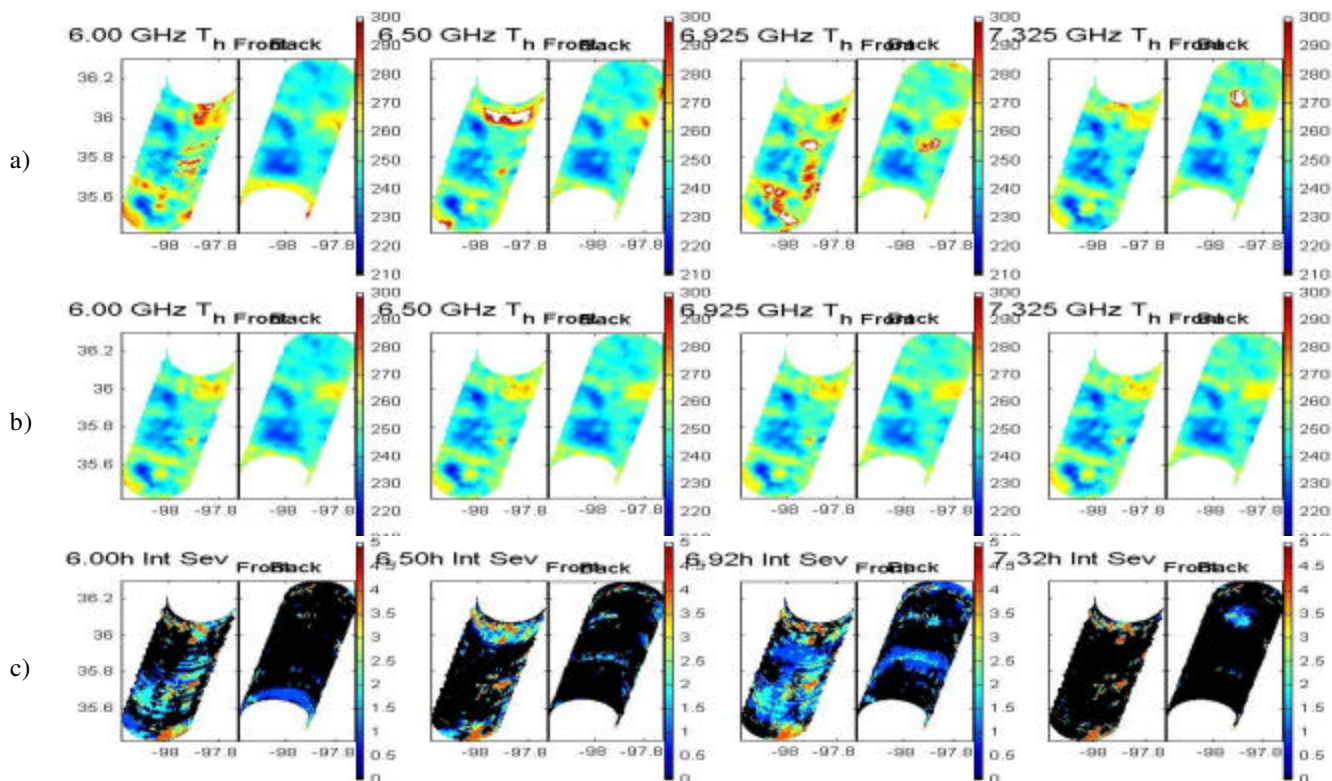


Figure 2. PSR/C C-band maps from a swath segment observed during SP99 on July 14, 1999 over central Oklahoma: a) raw calibrated brightness maps for front and back looks for the four PSR/C subbands, b) interference-corrected maps using the spectral subband algorithm of Figure 1, and c) interference severity maps (0-5) showing the level of interference and correction.